ATOMISTIC MODELING IN POLYMER NANOCOMPOSITE SYSTEMS – APPLICATIONS TO PROCESSING AND MECHANICS OF MULTI-SCALE MATERIALS

R. Mohan[*] and A. Kelkar

Joint School of Nanoscience and Nanoengineering, 2907East Lee Street, North Carolina A&T State University, Greensboro NC 27401, USA
*rvmohan@ncat.edu

Keywords: Atomistic modeling, material interactions, hybrid composites, nanocomposites

Abstract
The behaviour of hybrid and nancomposites is influenced by the material interactions during processing, and by the damages/defects in the molecular configurations of the associated constituent materials. This paper presents the molecular dynamics modelling of the material interactions that exist during the processing of an epoxy-glass fibre-alumina nano particulate hybrid composite. Modeling analysis results indicate that functionalization of alumina with silane T2MEVS (Tris2-Methoxyethoxy Vinyl Silane) improved the silane-alumina adhesion with epoxy compared to the alumina-epoxy adhesion. In addition, the effects of the SWCNT molecular structure defects on the predicted mechanical properties of the CNT-Epoxy nano composite are presented. Modeling analyses indicate that damages/defects in the SWCNT structure lead to a reduction in the CNT-Epoxy nanocomposite properties.

1 Introduction

Hybrid and nano composites are formed with material phases at varying length scales, and include nano material constituents. The behaviour of these composites is influenced by the material interactions during processing, and by the damages/defects in the associated constituent nano materials. Low length scale modelling based on the atomistic, molecular structures provides an insight into the molecular level interactions that exist, and their influence on the associated composite properties. Such modelling can also provide predictive properties and an understanding of the atomistic level behaviour. This paper discusses the role of atomistic modelling and simulations with a focus on applications to two multi-scale, hierarchical nanoengineered composite material systems consisting of alumina nanoparticulate, epoxy fibre hybrid composites and carbon nanotube epoxy nanocomposites.

2 Molecular Modeling in Alumina Nanoparticulate Hybrid Composites

Hybrid epoxy fibre composites with alumina nanoparticles are formed with nanomaterial integration via either fibre or resin modification [1]. To improve the compatibility of inorganic alumina with epoxy polymer, alumina was functionalized using silane (Tris-2-methoxyethoxy-vinyl-silane). The mode-I fracture toughness values are found to be significantly higher with functionalized alumina in our experimental investigations. The

macro level material behaviour depends on the material interactions at the fundamental molecular level. In this case, the functionalization of alumina with silane changes the material interface configuration to silane-alumina from the original epon-alumina altering the molecular interfacial energy across the material configurations. Molecular dynamics modelling for the interaction energy of different material interfaces in the hybrid epoxy fibre composite that exist due to functionalization during the processing are studied and correlated. Recent advances in the use of computational simulation of theoretical models for ab-initio and force-field parameterization in molecular modeling of polymeric systems have motivated extensive research work in these areas [3-7].

The primary and secondary constituent material molecular structures involved are: 1. Epoxy resin based on epoxy end chain with bisphenol-A inner organic group, 2. Curing agent butan-diamine, an amorphous organic compound, 3. Alumina (Aluminium Oxide, Al_2O_3), an inorganic compound, 4) Tris-2-methoxyethoxy-vinyl-silane, an organo-functional group linked to vinyl silane. The cured molecular models of epoxy consisting of EPON™ 9554 and curing agent butan-diamine (BDA) were developed using Accelrys Material Studio (Accelrys MS) development tool. The molecular models are configured for various degrees of networking of the cross-linked structure. Molecular dynamics models of the silane agent tris-2-methoxyethoxy vinyl silane (T2MEVS) and un-bonded alumina structure were also developed using Accelrys MS. A parameterized COMPASS (Condensed-phase Optimized Molecular Potentials for Atomistic Simulation Studies) force-field term was employed. Simulations employed canonical (NVT, constant number of atoms, constant volume and constant temperature) thermodynamic state variable using the Velocity Verlet algorithm numerical scheme for the dynamic analysis.

2.1 Molecular Modeling of Material Constituents

2.1.1 EPON™ 9554, BDA and cured Epoxy

EPON™ 9554 is an epoxy end chain (di-epoxy) with a bisphenol-A inner organic group. The epoxy structure is an amorphous polymer with high propensity for cross-linking polymer chain to form a thermoset polymer compound. The di-epoxy ends provide the potential for polymerization cure by cross-linking reaction. Figure 1 shows the molecular/ chemical structure of the epoxy and BDA. The molecular weight of epoxy is 340.419 amu.
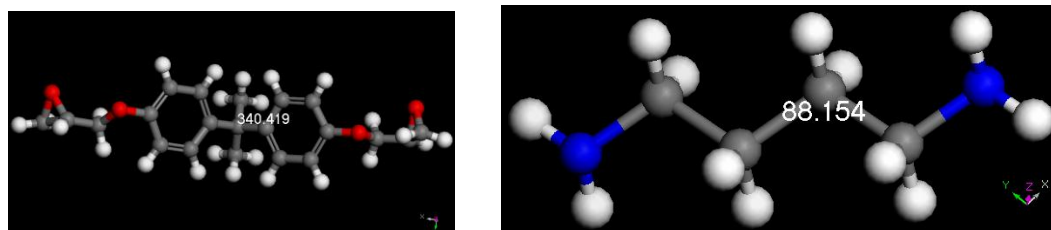

Figure 1. Molecular Structure (Left to Right) Epoxy Resin, BDA

The curing compound used in the processing is butan-diamine (BDA). It is a non-aromatic polyamine and an amorphous organic compound. It is very volatile readily breaking down to give off toxic ammonia gas. The end di-amine chain serves as a cross-linker in a complex polymeric structure due to its ability to give off its hydrogen to the epoxy molecule to form a hydroxyl and bond to the carbon atom in the epoxy ends. The molecular weight of butan-diamine is 88.154 amu.

Molecular dynamics models of the cured epoxy were built using the configurations for the epoxy resin chemically bonded with BDA curing agent. Using a stoichiometric ratio of 1:1 to concur with the mixing ratio during processing, molecular unit consisting of 4, 6 and 8 molecules of epoxy and curing agent were developed. Rhomboid, triangle and rectangular structures of cured epoxy structure with 4, 6 and 8 molecule cells were built and studied. These epoxy cell structures are shown in Figure 2.
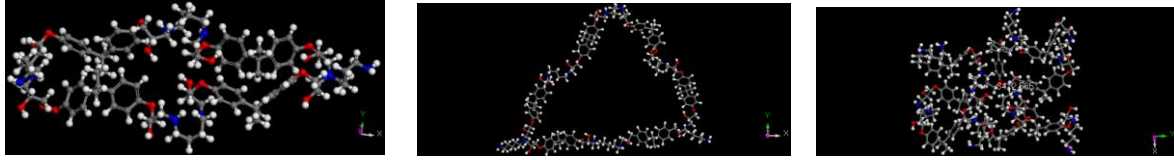

Figure 2. Rhomboid, Triangle and Rectangle (Left to Right) Molecular Configurations of Cured Epoxy Structure

2.2 Atomistic Analysis of Material Constituent Interactions

The energy interaction between the molecular configurations of the material constituents were performed using layered molecular cell configurations. Molecular cells used are interfaced lattice structure placed in a layered vacuum slab. The two molecular cells of any two primary material constituents are interfaced with each other to form a layered cell. The layered cells used in this study are: Epoxy – Alumina representing the interface material interaction between the epoxy and non-functionalized alumna; Silane-Alumina, representing the material interaction between functionalized alumina and epoxy resin; Epoxy-Silane and Epoxy-Epoxy layered configurations were studied as control simulations. Figure 3 presents the four different configurations of molecular interactions.
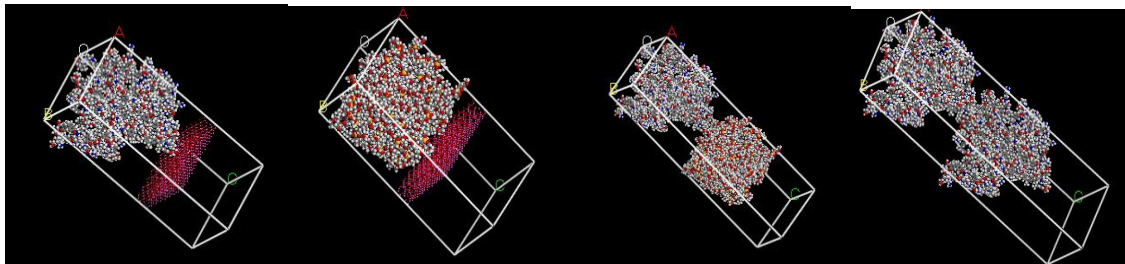

Figure 3. Molecular Layer Configurations
(L-R: Epoxy-Alumina (non-functionalized interaction); Silane-Alumina (functionalized interaction); Epoxy-Silane and Epoxy-Epoxy)

2.3 Surface Interaction Energy of Constituent Material Interactions

Total potential energies are obtained after canonical molecular dynamics for the periodic cells of the layered molecular models shown in figure 3. The potential energy of the four material interaction configurations shown in figure 3 is used to compute the interface energy of the interactions. The interface energy between two material constituents A and B is computed for a layered cell that contains these two molecular material components. The total energy of the layered cell is the sum of the energy of each component and the energy at the interface. The surface energy at the interface of a layered molecular cell is thus defined by

$$E_{A-B} = E_T - (E_A + E_B)$$

(1)

Subscripts A and B denote two molecular material models in a layered cell, E_T is the total energy of the entire layered cell, while E_A and E_B are the energies of the individual molecular models, and E_{A-B} defines the energy at the interface. The interaction energy at the interface is determined by the surface interaction energy per unit area and is given by

$$\gamma = \frac{E_{A-B}}{NS} \tag{2}$$

In the above equation, N is the number of moles and S is the interfacing lattice area in squared angstroms. The COMPASS force-field term exclusively formulated for the covalent bonded compounds is used for the determination of total potential energy using the Discover module in Accelrys.

In the simulation for organic-inorganic interactions, the energy contribution of alumina is negative due to the neglecting of the ionic bond interaction in the non-bonded Alumina molecular models employed. All the interactions involving alumina neglected ionic bond interaction consistently. This results in a net negative energy of the system. This net repulsion is indicative of the energy between the alumina with either epoxy or silane T2MEVS that does not include the ionic bond interaction within alumina. Both employed consistent non-inclusion of ionic bond interaction between alumina molecules. Complete details of the molecular modeling are presented in reference [8].

Figure 4 presents the comparison of the interface energy of epoxy-Alumina (non-functionalized interaction) and silane-alumina (functionalized interaction) interfaces for 5 and 10 cured epoxy molecular units. The energy level comparisons show silane to have improved adhesion to alumina with a higher energy level than a direct EPON-alumina.
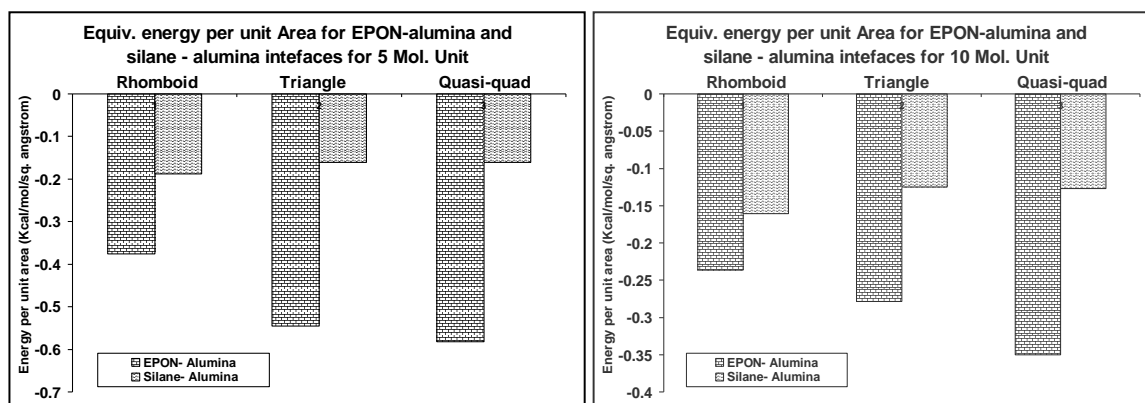

Figure 4. Comparison of Epoxy-Alumina and Silane-Alumina Interfaces Energies

The interaction of epoxy and silane agent T2MEVS were studied with a canonical ensemble by molecular dynamics simulations in a molecular vacuum slab. Equivalent cell sizes were used for these simulations. The equivalences used are epoxy interacting with epoxy as a control and epoxy interacting with an equivalent silane cell. Table 1 presents the computed interface energy for the epoxy-epoxy and epoxy-silane configuration using a 10 cell epoxy configuration for the three cured epoxy molecular configurations (figure 4). There was a very little difference in interface binding energy between epoxy-epoxy and epoxy-silane configurations indicating that these two material constituents are equally compatible.

Epoxy Structure	Rhomboid	Triangle	Quasi-Quad
Epoxy-Epoxy Energy (KCal/ Mol/ $\hat{A}^2$)	-0.00744	-0.00737	-0.00838
Epoxy-Silane Energy (KCal/ Mol/ $\hat{A}^2$)	-0.00835	-0.00895	-0.01103

Table 1. Interface binding energy for Epoxy – Epoxy and Epoxy – Silane

It can be inferred from figure 4 that silane-alumina interface showed better adhesion compared to epoxy-alumina. This improved adhesion of silane-alumina can potentially be attributed to the increase in fracture toughness energy release rate values with functionalization that were obtained for the mode-I fracture behavior of the alumina nano-particulate epoxy glass hybrid composite laminates in the experimental studies [2]. It can be inferred from the interaction energy of the material constituents obtained through molecular modeling that the functionalization employed during the processing improves the chemical affinity between the constituent materials involved. This can be a potential contributor to the improved mode-I fracture toughness values with functionalization, observed in the macroscopic experimental studies.

3 ATOMISTIC MODELLING OF EPOXY-CNT NANOCOMPOSITE

Computational techniques such as molecular dynamics (MD) simulations have emerged as an alternative to the traditional experimental and theoretical methods of estimating mechanical properties of the Epoxy – Carbon Nanotube composite systems. However, differences have been observed between results obtained from experiments and those obtained from MD simulations with the experimental results being lower. The effect of carbon vacancy defects in the single wall carbon natotube (SWCNT) on the Young's modulus of the EPON 862-DETDA-SWCNT composite evaluated through molecular dynamics simulations performed with Accelrys and Materials Studio are discussed and presented. Since their discovery, Carbon nanotubes (CNT) have gained significant attention because of their superior chemical, mechanical and thermo-physical properties. Inclusion of CNTs in polymer matrices have shown significant improvement of properties compared with the properties of the parent polymers, however, defects in these CNTs have also been observed to have detrimental effects on the mechanical properties of the composites [9-11].

3.1 Modelling Methodology

All molecular models were created and simulated in Materials Studio/Discover by Accelrys. The potential energy of the models was characterized by the COMPASS force field with the non-bond energies characterized by the Vander Walls and Coulomb's interactions. Figure 5 shows the molecular structures of EPON 862 and DETDA.
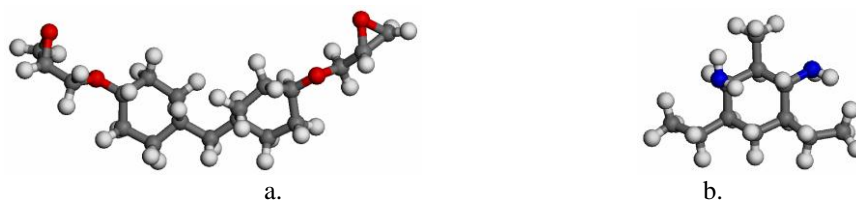

a.   b.

Figure 5. (a) EPON 862 and (b) DETDA molecular structures from Materials Studio

The recommended weight ratio of EPON 862 to DETDA for a fully cured composite during processing is 100:26.4. Because EPON 862 has a molecular weight of 312, and DETDA has a molecular weight of 178, the molecular ratio of the fully cured composite was approximated to 2 molecules of EPON 862 to 1 molecule of DETDA. The fully cured composite was therefore constructed with 8 molecules of EPON 862 and 4 molecules of DETDA.

Three nanocomposite models with SWCNT weight percentages between 7% and 12% are studied. The three molecular models of the defective SWCNT (DSWCNT) cured epoxy system used had the following configurations and weight percentages:

1. 3 unit cells of DSWCNT and 2 fully cured epoxy matrix corresponding to the CNT weight percentage of 11.28-11.58% at this configuration.
2. 4 unit cells of DSWCNT and 3 fully cured epoxy matrix corresponding to the CNT weight percentage of 10.34-10.49% at this configuration.
3. 4 unit cells of DSWCNT and 4 fully cured epoxy matrix corresponding to the CNT weight percentage of 7.95-8.08% at this configuration.

The models were minimized to obtain the lowest energy configuration. A cascade of the steepest descent minimization method and the Fletcher-Reeves method were used for the minimization. The minimized models were then equilibrated with the NVT ensemble for 100ps at 298 K. A sample simulation cell of cross linked epoxy and CNT is shown in Figure 6.
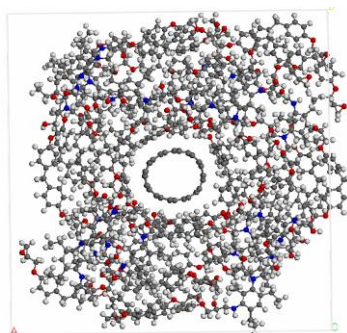

Figure 6. Simulation cell showing the CNT embedded in the fully cured epoxy matrix

Simulated annealing was used to mimic the curing cycle of EPON 862-DETDA-SWCNT composite and to ensure that the final configuration had the lowest energy possible. A characteristic property of simulated annealing is lowering the temperature slowly in stages to allow thermal equilibrium to be attained at each stage. The cell was heated to 498 K, and the temperature was dropped to 298 K in steps of 10 K using the NPT ensemble with a specified pressure of 0.0001 GPa (1 atm). MD simulations were run at each temperature for 200 ps with a time step of 1 fs. The final structure of each step was used as the starting structure of the next step. The density was noted at each step. At 298 K, an analysis of the elastic properties was performed by saving 10 trajectories and using them for the estimation.

3.2 Defect Types

The effect of 2 and 4 carbon vacancy defects in the SWCNT on the mechanical properties of the nanocomposite are investigated. Incorporation of the 2 defects was accomplished by removing two adjacent vertical carbon atoms on one side of the nanotube. Because of the short length of the nanotube removal of the 4 defects was accomplished by removing two adjacent vertical carbon atoms on opposite sides of the nanotube. Figure 7 shows an image of the DSWCNT with 2 adjacent carbon atoms removed
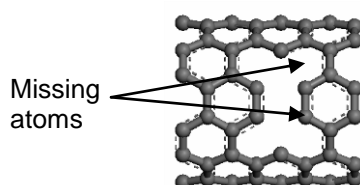

Figure 7. SWCNT with 2 missing adjacent carbon atoms

With the SWCNT having a density of 1.9 g/cm^3 and the epoxy resin having a density of 1.2 g/cm^3, the rule of mixtures densities of the composites were calculated. To obtain the Young's modulus at the exact densities for each of the models, simulated annealing runs were conducted at three different lattice configurations for each model and interpolated to the exact density. The corresponding Young's modulus was then evaluated.

3.3 Predictive Mechanical Property of Epoxy – CNT Nano Composite

Table 2 presents the predicted mechanical properties of the Epoxy – CNT nanocomposites obtained from the molecular dynamics simulations. This can be interpreted as follows: For the 11.87% SWCNT composite, introduction of 2.78% of defects into the SWCNT resulted in 17.9% overall reduction in the Young's modulus, while introduction of 5.56% of defects into the CNT resulted in 29.6% reduction in the Young's modulus. For the 10.67% SWCNT composite, introduction of 2.08% of defects into the SWCNT resulted in 15.7% overall reduction in the Young's modulus of the nanocomposite while introduction of 4.17% of defects into the CNT resulted in 25.1% reduction in the Young's modulus of the composite. For the 8.24% SWCNT composite, introduction of 2.08% of defects into the SWCNT resulted in 13.6% overall reduction in the Young's modulus of the composite while introduction of 4.17% of defects into the CNT resulted in 21.9% reduction in the Young's modulus of the composite.

CNT weight % (No defect)	Young's Modulus [GPa]	
	% reduction with 2 defects in composite	% reduction with 4 defects in composite
11.87	17.9 (2.78% defects in CNT)	29.6 (5.56% defects in CNT)
10.69	15.7 (2.08% defects in CNT)	25.1 (4.17% defects in CNT)
8.24	13.6 (2.08% defects in CNT)	21.9 (4.17% defects in CNT)

Table 2. Percentage reduction in Young's modulus with the introduction of defects

Atomistic modelling for the predictive properties of epoxy-CNT nanocomposites clearly indicate that 2 carbon vacancy defects in the SWCNT resulted in a reduction in Young's modulus of between 13-18% when compared with the defect free CNT – epoxy nanocomposite molecular models, while four vacancy defects resulted in a reduction of Young's Modulus value between 21-30% when compared with the defect free CNT – epoxy nanocomposite molecular models. There is a great potential for the damage and introduction of such defects during the experimental processing of CNT – Epoxy nanocomposites. This coupled with the multiple orientations of the CNT distribution in the macro specimens potentially contribute to the disparity seen in the predictive molecular modelling properties and the experimental macro properties of these nanocomposites.

4 CONCLUDING REMARKS
The applicability of the molecular dynamics modelling simulations in the processing and mechanics of hybrid composites are discussed and presented. In the first system, molecular modelling analysis of interface energy of the material constituents that exist during the processing of a hybrid epoxy-glass fibre-alumina nanoparticulate hybrid composite indicate

that silane-alumina interface showed better adhesion compared to epoxy-alumina. This improved adhesion of silane-alumina can potentially be attributed to the increase in fracture toughness energy release rate values with functionalization that were obtained for the mode-I fracture behavior of these composites experimentally [2]. In the second system consisting of Epoxy-CNT nanocomposite, the molecular defects in the CNT showed a reduction in the predicted mechanical (Young's Modulus) properties of the nanocomposite. These two studies clearly elucidate the applicability of low length scale modelling based on the molecular material structures to provide an insight into the molecular level interactions that exist, and their influence on the associated macro composite properties. These two studies elucidate the applicability of low length scale modelling based on the molecular material structures to provide an insight into the molecular level interactions that are influenced by functionalization during processing and molecular defects that influence the mechanical properties of nanocomposites.

References

[1] Akinyede O., Mohan R., et al. Processing and Thermo-Physical Characterization of Alumina Particulate Reinforced 3-Phase Hybrid Composite Material System, *Journal of Advanced Materials*, July 2010.

[2] Akinyede O., Mohan R., et al. Static and Fatigue Behavior of Epoxy/Fibre Glass Composites Hybridized with Alumina Nanoparticles, *J. Composite Materials*, 43(7), 769-781 (2009).

[3] Gou J., Liang Z., Zhang C., Wang B. Computational Analysis of Effect of Single-Walled Nanotube Rope on Molecular Interactions and Load Transfer of Nanocomposites, *Composites-Part B*, 35, 524-533 (2005).

[4] Wong M., M. Paramsothy M., Xu, XJ., Ren Y., Li, S., Liao. Physical Interactions at Carbon Nanotube-Polymer Interface, *Polymer*, 44(25), 7757-7764 (2003).

[5] Frankland S.J.V., Caglar A., Brenner D.W., and Giebel M. Molecular Simulation of the Influence of Chemical Cross-Links on the Shear Strength of Carbon Nanotube-Polymer Interfaces, *The Journal of Physical Chemistry B*, 106(12), 3046-3048 (2002).

[6] Frankland S.J.V., and Harik V, Analysis of Carbon Nanotube Pull Out from a Polymer Matrix, *Surface Science Letters*, 525, 303-308 (2003).

[7] Pan, E., Zhu, R., and Roy, A.K. Molecular Dynamics Study of the Stress-Strain Behavior of Carbon Nanotubes Reinforced EPON™ 862 Composite, *Material Science and Engineering A*, 44, 51-57 (2007).

[8] Mohan, R., Okinyede, A. "Molecular Dynamics Simulations and Analysis of Material Interactions in Alumina Particulate Hybrid Composites, *AIAA-2008-2097*, AIAA Structural Dynamics and Materials Conference, Chicago, IL (2008).

[9] Mielke S. L., Troya D., Zhang S., Li J. L., Xiao S., Car R., Ruoff R. S., Schatz G. C., Belytschko, T. The role of vacancy defects and holes in the fracture of carbon nanotube, *Chemical Physics Letters*, 390, 413-420 (2004).

[10] Mielke L. S., Zhang S., Khare R., Troya D., Ruoff R. S., Schatz G. C., Belytschko T. Mechanics of Defects in Carbon Nanotubes: Atomistic and Multi-Scale simulations, *Physical Review B*, Volume 71, (2005) 115403.

[11] Li Z., Wang C. Y., Ke S. H., Yang W., First principles study for transport properties of defective carbon nanotubes with oxygen adsorption, The European Physical Journal B, Volume 69, (2009) 375-382.